Silicon (2017) 9:165–172
DOI 10.1007/s12633-015-9386-4

ORIGINAL PAPER

Mechanical Properties of Artificial Stones Produced from Sludge of Stone-Cutting Factories (SSCF): The Effects of Nano-fillers (aTiO$_2$ and ZnO Nanoparticles)

Nasim Sarami[1] **· Leila Mahdavian**[1]

Received: 10 February 2015 / Accepted: 26 November 2015 / Published online: 19 February 2016

Abstract The aim of this study is to present the advantages of artificial stone production from the sludge of stone cutting factories (SSCFs), which is a self-cleaning and low-cost process, in Lorestan province, Iran. The basic formulation of artificial stone is the sludge stone: 50 % of the weight (wt.%) of sludge stone is cement. 12 wt.%, 25 wt.%, and 7 wt.% of the cement consists of unsaturated polyester resin liquid (UPR), water, and, filler respectively. The filler itself is made up of micro-silica and different amounts of anatase TiO_2-NP and ZnO-NP. Nanoparticles lead to hydrophobicity, the analysis of oil stains, the elimination of bad odor, the sterilization and self-cleaning of artificial stone. The production of artificial stone via this method is pressure-resistant, highly flexible, resistant to freezing and scrapes, lightweight, capable of being cut and formed with a low thickness, and self-cleaning compared to the natural stone.

Keywords Sludge of stone cutting factories (SSCFs) · Artificial stone · Micro-silica · aTiO$_2$-NPs · ZnO-NPs · Unsaturated polyester resin liquid (UPR) · Cement

1 Introduction

Currently, due to such factors as the poor quality of natural stones, short-term adhesive materials in the facade of buildings, high moisture absorption, low resistance, few mining resources, and environmental issues, consumers are looking for stones with superior strength and quality and cheaper prices [1–3]. This tendency can be accounted for by other reasons like the lack of diversity in design and color, the penetration of contamination into the stone tissues, and stone opacity in the long term [4]. Artificial stones with a good quality and reasonable price can be an appropriate substitute for natural stones. The price of artificial stones is low due to benefiting from useless stones and low costs of excavation and transportation [5].

Travertine and marble reserves in Iran are around 450 and 44 million tons, respectively. In Lorestan province, Iran most mines are travertine [4]. Thus, more than 40 % of the ore mined is wasted and dumped around the cities (Fig. 1).

Chemical analyses of travertine wastes are as follows for the production of the synthetic artificial stones: CaO, SiO_2, FeS_2, MgO, Na_2O, loss on ignition (LOI), clay (K_2O, Al_2O_3, and Fe_2O_3), sulfate, and organic materials [6]. Waste travertine has the following properties: acceptable resistance, low hardness, ability to be polished and cut, high strength and formability, having crystals, high density, beauty, porosity for full adherence to grout, ease of access, impossibility of altering its reserves, variety of colors, and reasonable price compared to that of natural stone [7–9]. Due to the porosity of the stone, having a lot of waste is inevitable when cutting and polishing, which is an environmental problem for this region. The aim of this study is to reuse the sludge of stone cutting factories and produce artificial stones which are highly resistant, self-cleaning, dust escaping, and hydrophobic. For this purpose, the addition of inorganic nanoparticles and some other organic materials are employed [10–12]. Nanoparticles of titanium dioxide and zinc oxide are combined in artificial stone made from

✉ Leila Mahdavian
mahdavian_leila@yahoo.com; Mahdavian@iau-doroud.ac.ir

1 Department of Chemistry, Doroud Branch, Islamic Azad University, P.O. Box: 133, Doroud, Iran

Fig. 1 **a** Stone quarry of Doroud, **b** stone cutting factory and **c** waste and sludge of stone cutting factory (SSCF)

natural minerals and unsaturated polyester resin (UPR), can be added to the molecular structure in order to modify the cement (crystalline) and cause a polymerization reaction. By changing the molecular structure, compounds are produced with a strength 2 to 3 times more than that of the concrete and 2 times more than that of the natural stones, a good adhesion and high compressive strength, low moisture absorption, lack of blur penetration into the stones, and a self-cleaning nature.

2 Experimental

2.1 Materials and Devices

The aTiO$_2$-NP and ZnO-NP are the products of MERK, Portland cement type II; this type of cement has normal properties, meaning that the setting time is low and the cement is resistant to sulfate compounds. In this cement, the amounts of tri-calcium silicate decrease while those of di-calcium aluminates and di-calcium silicate increase [13]. Other materials such as unsaturated polyester resins (UPR) and micro-silica powder are produced by MERK, and the sludge of stone cutting factories (SSCFs) is produced in a factory in the outskirts of Doroud city, Iran (Fig. 1).

The devices required in this study are as follows: a press or kicker, a mixer and a meter setting (Joint Stars Group Limited). The sizes of templates are 5 × 5 × 5 and 16 × 4 × 4 cm^3. In the light microscope the condenser, abb, N.A. 1.25, adjustable aperture, and aperture center can be adjusted. In the electric component the input voltage is AC85-265 V and 50/60 Hz. The output voltage is DCI.2-6 V. 6V/20 W, and there is a halogen lamp rotation potentiometer with power switch fuses of 2A 5*20.

The compressive strength device (product of Toni Tecknik Germany number PR41004) has the following specifications: serial number of 1543-03, pressure of 288bar, piston strokes of 60 mm, piston diameter of 115 mm, and Toni tecknik Gmbh - Gustav - Meyer - Allee25 - D-13355 Berlin. The flexural strength device (product number, Toni Technik Germany RB421002) has the following characteristics (Fig. 2): serial number 2061-03, pressure of 125 bar, piston strokes of 30 mm, piston diameter of 32 mm, and Toni Technik Gmbh–Meyer–Allee 25–D–13355 Berlin.

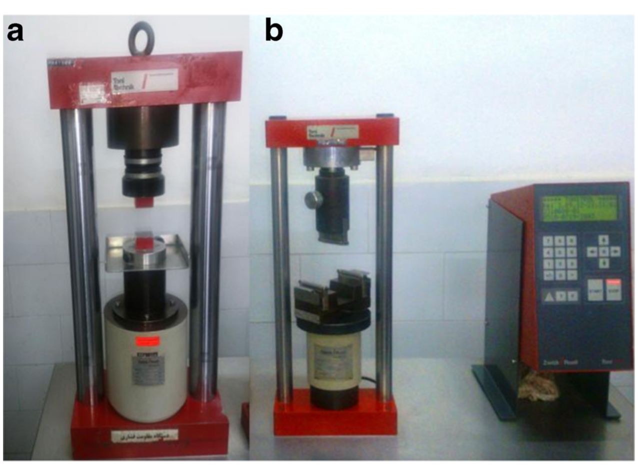

Fig. 2 Scheme of: **a** compressive strength and **b** flexural strength device

2.2 Methods

To test the samples templates with the following sizes were used: 5 × 5 × 5 and 16 × 4 × 4 cm^3. According to the formulation of Table 1, the composition of the base of artificial stone was determined. The percentage composition of cement weight (wt.%) was the determined ratio to wt.% of SSCF, and the other materials were determined to the wt.%

Table 1 The formulation of composition of artificial stone base

Material	Weight %
SSCF	Same as mold
Cement	50 wt.% of SSCF
Unsaturated polyester resin liquid (UPR)	1–15 wt.% of cement
H_2O	20–30 wt.% of cement
Micro Si or $CaCO_3$	7 wt.% of cement

Table 2 The basic formulation of artificial stone from SSCF in different combinations

Samples	Sludge of stone cutting factory (SSCF)	Cement (C)		Water		Unsaturated polyester resin (UPR)	
	g	wt.% to SSCF	g	wt.% to C	g	wt.% to C	g
1	177	50	88.5	30	26.55	10	8.85
2	177	50	88.5	25	22.13	12	10.62
3	177	50	88.5	20	17.70	15	13.27

of cement. It should be noted that the mixes or the formulations of the samples were selected in accordance with ACI 211.1-91 Standard of America [14].

2.2.1 Methods of Preparation of Artificial Stone

The cement was initially weighed and was equal to 50 wt.% of SSCFs, while the water was 20–30 wt.% of the cement. The water and the cement were mixed in a blender stirring for 1 min at low rpm. The SSCF, the unsaturated polyester resin liquid (UPR) and the filler were added to a mixture of water and cement (7 wt.% micro Si or calcium carbonate for minimizing pores), and stirred for 1.5 min at high rpm. The mixture was then ready for molding.

2.2.2 The Molding Method of Artificial Stone

After cleaning the templates, greasing them, and filling their seams, they were installed on a kicker device. A layer of the mixture was poured into a template and the kicker machine started, and the mixture received 60 hits Afterwards, the second layer was poured and then was hit 60 times with the mixture set to air leak. The templates were then put in a humidity bath for 24 h ($\theta = 30\,^{\circ}$C and $\omega = 90$ %). The concrete composite showed better resistance in the absence of water. Table 2 shows samples with various combination percentages of water and unsaturated polystyrene resin (UPR). The mechanical properties of the artificial stones are shown in Table 3.

2.2.3 Compressive Strength Test

The UK test standards BS EN 12390-1: 2000 and BS EN 12390-2: 2000 were carried out [15]. The samples of templates were placed after being dried on the compressive strength device divided into two pieces.

2.2.4 Flexural Strength Test

The tensile strength test applying axial tension was done on the samples. The problem was the force exerted in line with the axis due to the shape of the templates. Therefore, the tensile strength, which was calculated via indirect methods in the bending test and the splitting (split-half) as per standard BS EN 14617-2: 2008, was conducted using the flexural strength [16–19]. The flexural strength is the modulus of rupture (MOR).

2.2.5 Test to Determine the Density and Water Absorption

The absorbed water is the maximum amount of water which is absorbed by the stones prepared when they are immersed in water at environmental temperature and pressure in accordance with international (BS EN 14617-1: 2005) standards [20].

2.2.6 Test to Determine the Abrasion Resistance

The method is based on scraping the upper surface of the artificial stone, using an abrasive (corundum containing alumina) under standards BS EN 14617-4: 2012. [21, 22].

Table 3 The mechanical properties of artificial stone

Samples	Compression strength testing $kg.cm^{-2}$	Flexural strength testing $kg.cm^{-2}$	Abrasion resistance $g.cm^{-2}$	Temperature resistance Thermal cycles	Density $g.cm^{-3}$	Water absorption
1	211.52	21.83	1.8	265	2.6	7.6 %
2	235.95	25.65	2.0	300	1.8	5.0 %
3	186.26	25.54	1.7	224	3.1	8.0 %

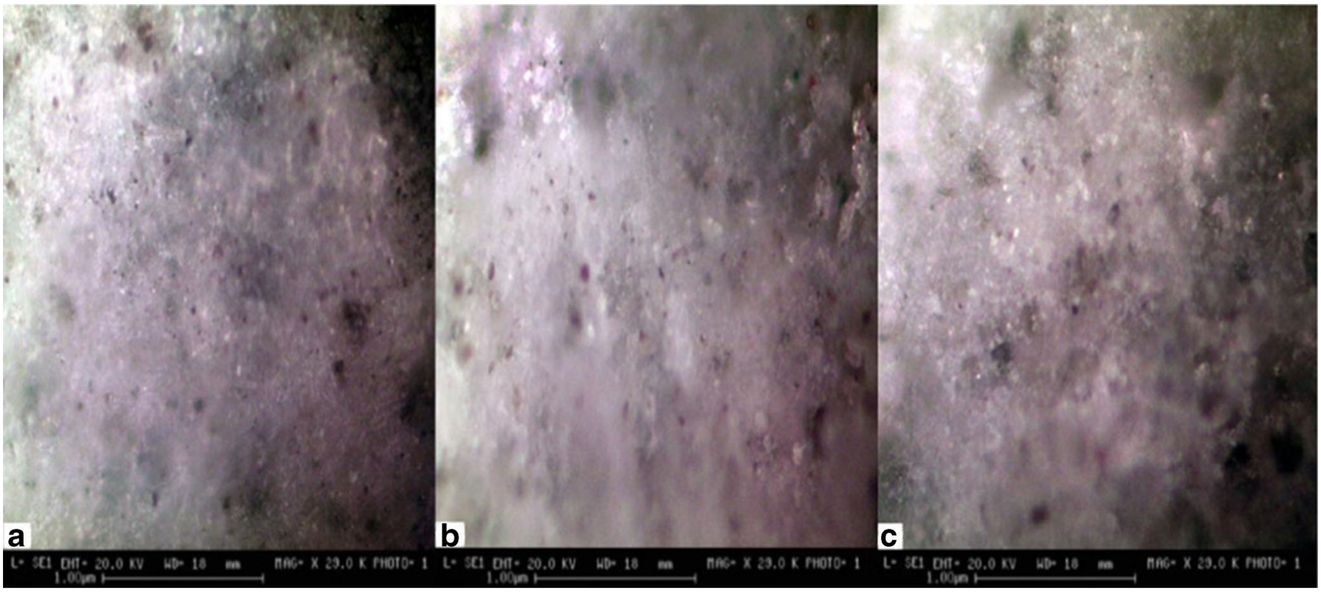

Fig. 3 The optical microscope images of the artificial stone with: **a** water is 30 wt.% of cement and UPRs are 10 wt.% of cement, **b** water is 25 wt.% of cement and UPRs are 12 wt.% of cement and **c** water is 20 wt.% of cement and UPRs are 15 wt.% of cement

2.2.7 Determination of Sensitivity to Changes in Appearance Produced by Thermal Cycles

The aim of this test is to evaluate probable changes in the stone (eye sensitivity to oxidation) which is affected by sudden changes of temperature (heat shock) by standards BS EN 16140: 2011 [23].

3 Results and Discussion

The important factors in the sludge formation and the waste decorative stones are as follows: a ton of stone from the mine is unsafe and consequently unusable when it reaches 50 % of the lesions, and the consumer must pay the price for each ton of stone twice. In addition, negligence in transporting the stones often causes the fracture of edges, cracks or scratches on the polished surface, and consequent lesions in the cutting by wire cutter in various parts of the broken stone.

The sludge of natural stones is the same as rock powder and does not need to be sieved. The best sample according to the results in Tables 2 and 3 is the second sample whose compressive and flexural strengths and other parameters are more than those of other samples. This sample was prepared by a formulation of 177 g of SSCF in which the cement is 50 wt.% of SSCF, the water is 25 wt.% of cement, and the UPR is 12 wt.% of the cement. Figure 3 shows the

Table 4 The mechanical properties of artificial stone from SSCF with wt.% of $a$$TiO_2$-NP filler

TiO_2-NP wt.%	Compression strength testing $kg.cm^{-2}$	Flexural strength testing $kg.cm^{-2}$	Abrasion resistance $g.cm^{-2}$	Temperature resistance Thermal cycles	Density $g.cm^{-3}$	Water absorption
5	419.81	77.81	3.01	415	1.74	4.13 %
15	591.22	82.05	3.42	426	1.71	4.09 %
25	625.62	98.17	3.65	439	1.68	4.07 %
35	679.71	121.29	3.87	465	1.66	4.00 %
45	735.71	138.92	3.91	487	1.62	3.81 %

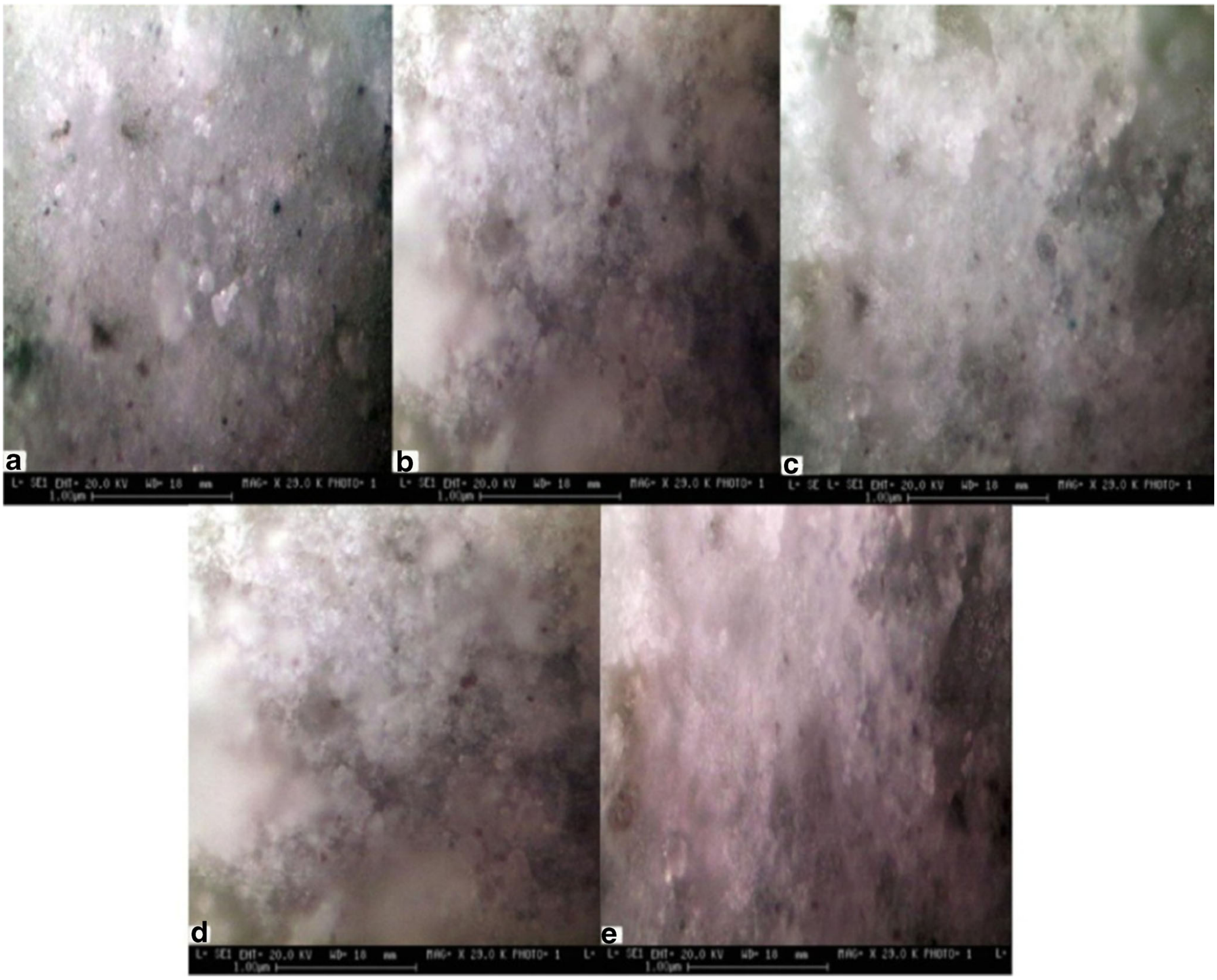

Fig. 4 The optical microscope images of the artificial stone with: **a** 5, **b** 15, **c** 15, **d** 35 and **e** 45 wt.% of *a*TiO_2-NP filler

optical microscope images ofthe artificial stone, produced via formulations in Tables 2 and 3. As seen in Fig. 3, the dark areas show porosity in the artificial stone, and its 25 wt.% of water and 12 wt.% of UPR are related to the cement which is less porous (part b in Fig. 3). To reduce the porosity of this sample, the fillers (micro Si and $CaCO_3$) were added to the second sample at 7 wt.% of cement. The results showed that the sample dried in the absence of a water pool,

Table 5 The mechanical properties of artificial stone from SSCF with wt.% of ZnO-NP filler

ZnO-NP wt.%	Compression strength testing kg.cm^{-2}	Flexural strength testing kg.cm^{-2}	Abrasion resistance g.cm^{-2}	Temperature resistance Thermal cycles	Density g.cm^{-3}	Water absorption
5	291.92	58.64	2.02	356	1.50	4.91
15	331.73	59.12	2.15	357	1.54	4.84
25	407.89	64.33	2.21	362	1.56	4.79
35	549.36	87.47	2.34	387	1.61	4.63
45	598.20	90.05	2.39	402	1.63	4.51

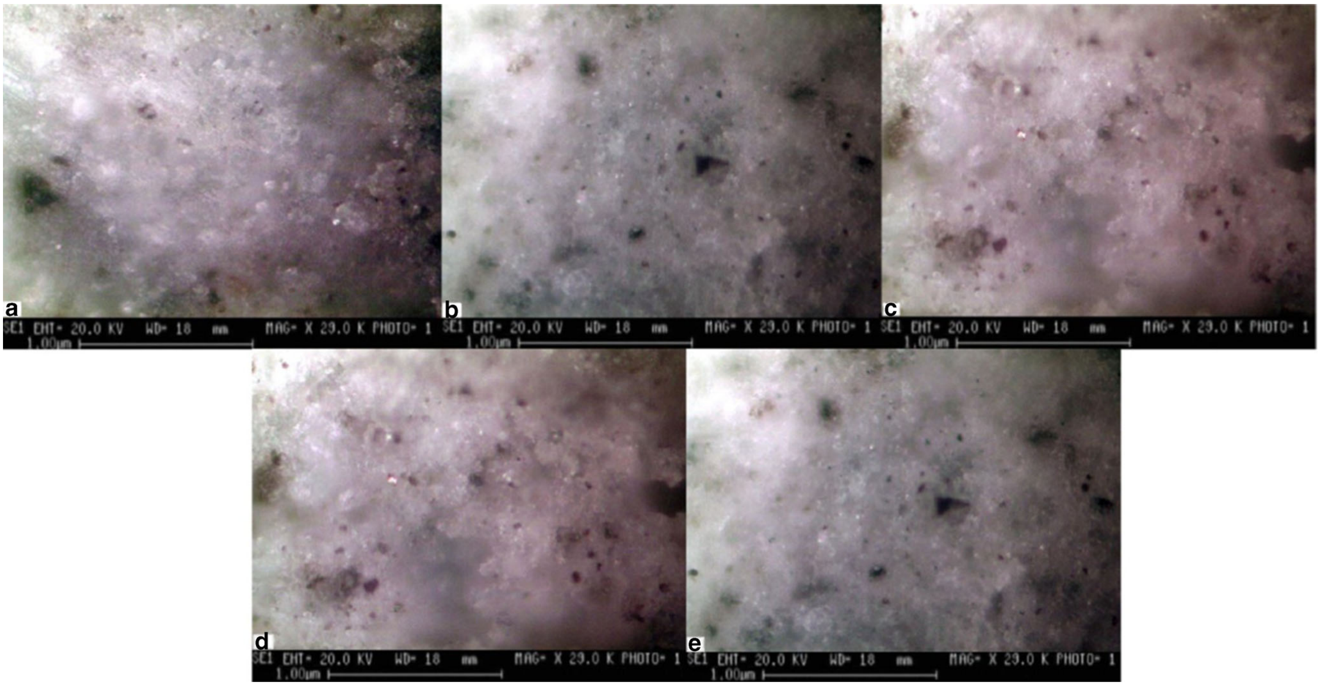

Fig. 5 The optical microscope images of the artificial stone with: **a** 5, **b** 15, **c** 25, **d** 35 and **e** 45 wt.% of ZnO-NP filler

and that the samples containing calcium carbonate (unlike concrete) were soft and disintegrated. However, the samples containing micro Si are less porous and stronger.

According to the previous results, the mechanical properties of this formulation are not satisfactory. To enhance the properties of micro-silica, the nanoparticles of $a\mathrm{TiO}_2$ and different types of ZnO in wt.% were added.

Table 4 shows the mechanical properties of these samples that are made with micro Si filler (7 wt.% of cement) with different percentages of TiO_2-NP. The obtained samples have smoother and glossier surfaces in comparison with the previous samples, and the compressive strength of the samples with different wt.% of $a\mathrm{TiO}_2$-NPs are better, and the coherent time of combination is lower than that of other samples. Figure 4 shows that for higher percentages of $a\mathrm{TiO}_2$-NP the porosity of the produced artificial stones decreases, whereas the linkage between the particles increases.

As seen in Fig. 4d and e, the porosity of samples is less, and they have a smooth surface. The mechanical properties of the samples increase (Table 4). Comparing Tables 3 and 4, the compressive and flexural strengths improve by increasing $a\mathrm{TiO}_2$-NP fillers.

Following the investigation, the zinc oxide nanoparticles were added instead of $a\mathrm{TiO}_2$ nanoparticles with the same percentage. The mechanical properties of these samples are shown in Table 5. By adding zinc oxide nanoparticles, the properties of the samples increase; however, the effect of

Table 6 The mechanical properties of artificial stone from SSCF with ratio of one to one from $a\mathrm{TiO}_2$ and ZnO-NP filler

TiO_2/ZnO-NP wt.%	Compression strength testing kg.cm^{-2}	Flexural strength testing kg.cm^{-2}	Abrasion resistance g.cm^{-2}	Temperature resistance Thermal cycles	Density g.cm^{-3}	Water absorption
5	348.18	61.53	2.27	378	1.41	4.53
15	534.15	69.93	2.32	392	1.48	4.48
25	590.07	85.98	2.45	409	1.49	4.41
35	629.88	115.83	2.60	421	1.52	4.37
45	658.93	126.13	2.87	463	1.58	4.29

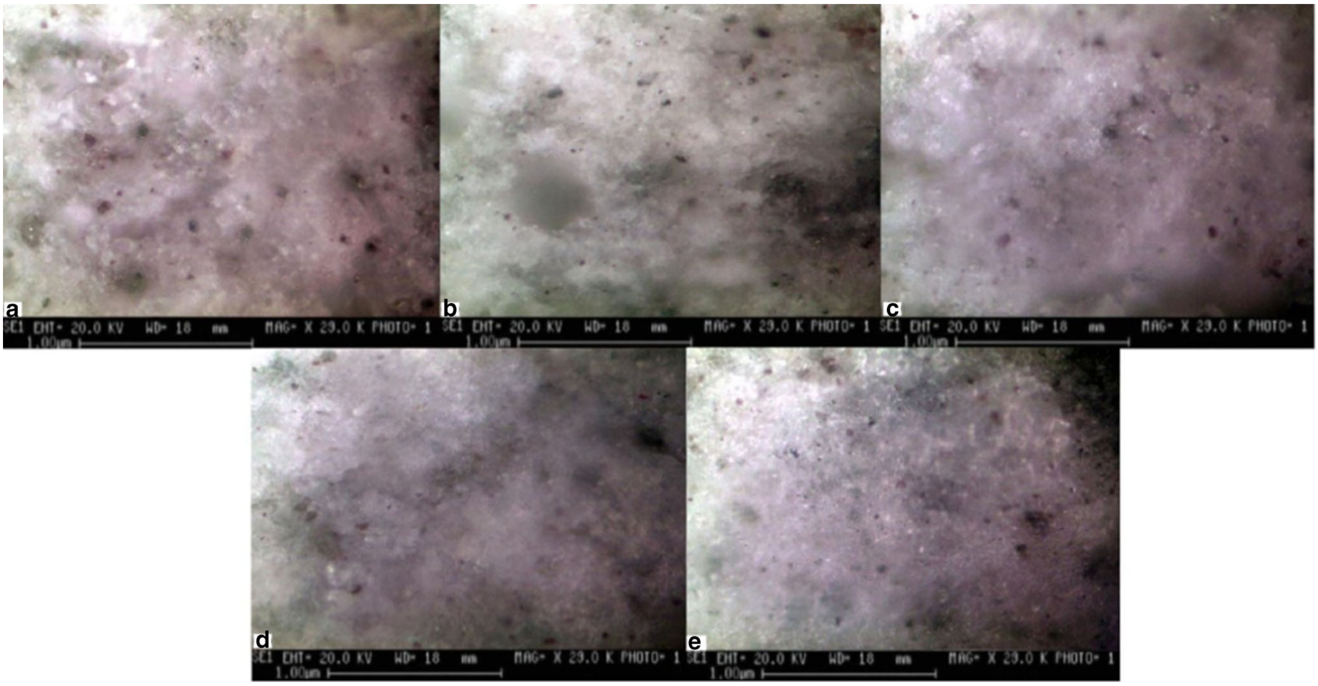

Fig. 6 The optical microscope images of the artificial stone with: **a** 5, **b** 15, **c** 25, **d** 35 and **e** 45 wt.% of TiO_2/ZnO-NP filler

$a$$TiO_2$ nanoparticles is boosted because it depends on the expansion of the surface and the crystal structure of titanium dioxide nanoparticles. As can be seen in Fig. 5, adding zinc oxide nanoparticles to artificial stone composition instead of titanium dioxide nanoparticles causes the reduction of mechanical properties. In addition, the porosity and voids in the stone increase.

At the end of the study, the titanium dioxide and zinc oxide nanoparticles were added to the artificial stone with a one-to-one ratio, and their mechanical properties are shown in Table 6. These samples show better properties compared to the samples containing zinc oxide nanoparticles. However, the ratio of mechanical properties is lower in comparison with the samples containing $a$$TiO_2$-NP.

As shown in Fig. 6, with an increase in $a$$TiO_2$/ZnO-NP in the percentage composition of the samples, the porosity drops. The porosity and voids in the samples are as follows:

$$aTiO_2 - NP < aTiO_2/ZnO\text{-}NP < ZnO\text{-}NP$$

All artificial stones were produced by the percentage combination of $a$$TiO_2$-NPs, and they had hydrophobic properties. Placing the samples in water, their surfaces did not absorb water. An amount of fatty oil was spread across the surface of the sample (45 wt.% of $a$$TiO_2$-NP and $a$$TiO_2$/ZnO), and the oil was analyzed in the sunlight, with the light having no effect on the oil level. These nanoparticles caused the hydrophobicity, analysis of oil stains, elimination of bad odor, and the sterilization of the self-cleaning artificial stones. The colors of artificial stones are being prepared and can be added by different pigments.

4 Conclusion

The aim of this study was converting the SSCFs to artificial stones. This process includes the production of self-cleaning artificial stones by SSCFs in Lorestan province, Iran by recovering natural resources which can be used in building materials, façades, and antique and composite paving stones.

The results show that since the percentage of travertine lesions is more in the wastes of factories and the properties of this kind of artificial stone have improved, the mechanical properties of artificial stones obtained from SSCFs of Doroud city, Iran are better. Adding $a$$TiO_2$ and ZnO nanoparticles to the artificial stones can cause some air pollutants to convert low-risk products such as NO_x to N_2 and O_2. The crystals of titanium dioxide nanoparticles have an excellent expansion of surface; therefore, adding this filler to the artificial stones causes the surface to be more smooth and glossy and show properties of water and dust escaping.

The characteristics of the produced artificial stones are as follows: resistance to abrasion, having long and useful life, low weight, and resistance to freezing. Besides, if the rocks are exposed to dirt, pollutants, fire, gravitational energy, and damp and wet environments, they are cleaned to the same quality.

Acknowledgments I would like to thank Islamic Azad University Doroud branch, for providing me with all the necessary facilities for this research.

References

1. Turgut P, Algin HM (2007) Limestone dust and wood sawdust as brick material. Build Environ 42(9):3399–3406
2. Alzboon KK, Mahasneh KN (2009) Effect of using stone cutting waste on the compression strength and slump characteristics of concrete. Int J Environ Chem Ecol Geol Geophys Eng 3(3):460–465
3. Masoud T (2015) Effect of using stone cutting slurry waste (Al-Khamkha) on the compaction characteristics of Jerash cohesive soil. Open J Civ Eng 5:214–219
4. Fahiminia M, Ardani R, Hashemi S, Alizadeh M (2013) Wastewater treatment of stone cutting industries by coagulation. Process Arch Hyg Sci 2(1):16–22
5. Al-Zboon K, Tahat M, Abu-Hamatteh ZS, Al-Harahsheh MS (2010) Recycling of stone cutting sludge in formulations of bricks and terrazzo tiles. Waste Manag Res 28(6):568–74
6. Sabah E, Aciksoz C (2012) Flocculation performanve of fine particles in travertine slime suspension. Physicochem Probl Miner Process 48(2):555–566
7. Mashaly AO, Shalaby BN, El-Hefnawi MA (2012) Characterization of the marble sludge of the Shaq El Thoaban industrial zone, egypt and its compatibility for various recycling applications. Aust J Basic Appl Sci 6(3):153–161
8. Joshi R (2013) Effect of using selected industrial waste on compressive and flexural strength of concrete. Int J Civ Struct Eng 4(2):116–124
9. Rehman W, Riaz M, Ishaq M, Faisal M (2014) Utilization of marble waste slurry in the preparation of bricks. J Pak Inst Chem Eng 42(1):2014
10. Al-Hamaiedh H (2010) Reuse of marble sludge slime in ceramic industry. Jordan J Civ Eng 4(3):264–271
11. Allam ME, Bakhoum ES, Garas GL (2014) Re-use of granite sludge in producing green concrete. ARPN J Eng Appl Sci 9(12):2731–2737
12. Al-Joulani N, Salah N (2014) The stone slurry in palestine from environmental burden to economic opportunities-feasibility analysis. J Environ Prot 5:1075–1090
13. Lea FM (1970) The chemistry of cement and concrete. Arnold, London
14. ACI COMMITTEE 211.1-91
15. Madandoust R, Alizadeh AM (2015) Assessing the effective parameters on normal strength concrete by core testing. J Automot Appl Mech 3(2):1–6
16. BS EN 14617-2: 2008, Agglomerated stone - Test methods - Part 2: Determination of flexural strength (bending)
17. EN 12372: 2007, Natural stone test methods - Determination of flexural strength under concentrated load
18. EN 14618: 2009, Agglomerated stone- Terminology and classification
19. EN 14617-16, Agglomerated stone - Test methods - Determination of dimensions, geometric characteristics and surface quality of modular tiles
20. BS EN 14617-1: 2005, Agglomerated stone - Test methods - Part 1: Determination of Apparent Density and Water Absorption
21. BS EN 14617-4: 2012, Agglomerated stone - Test methods - Part 4: Determination of the abrasion resistance
22. ISO 8486-1: 1996, Bonded abrasives - Determination and designation of grain size distribution - Part 1: Macrogrits F4 to F220
23. BS EN 16140: 2011, Natural stone test methods. Determination of sensitivity to changes in appearance produced by thermal cycles